Bioorganic & Medicinal Chemistry 21 (2013) 4614–4627

Contents lists available at SciVerse ScienceDirect

Bioorganic & Medicinal Chemistry

journal homepage: www.elsevier.com/locate/bmc

Synthesis of substituted diphenyl sulfones and their structure–activity relationship with the antagonism of 5-HT6 receptors

Alexandre Ivachtchenko [a,b], Elena Golovina [a], Madina Kadieva [a], Oleg Mitkin [a], Sergei Tkachenko [b], Ilya Okun [b,*]

[a] Department of Organic Chemistry and Department of Molecular Pharmacology, CDRI, 114401 Khimki, Moscow Reg, Russia
[b] ChemDiv, Inc. 6605 Nancy Ridge Drive, San Diego, CA 92121, USA

ARTICLE INFO

Article history:
Received 22 February 2013
Revised 5 May 2013
Accepted 15 May 2013
Available online 1 June 2013

Keywords:
Diphenyl sulfones
Serotonin 5-HT_6 type receptor
Molecular docking
Antagonists
Ligand

ABSTRACT

Substituted diphenyl sulfones (**10a**–**n**) were synthesised, and the structures were confirmed by NMR, LC–MS and X-ray crystallography. Their antagonistic activities towards 5-HT_6 receptor were assessed in a cell-based functional assay. Diphenyl sulfone **10a**, in spite of being the smallest and simplest known sulfonyl-containing 5-HT_6R antagonist, showed a strong potency (K_i = 1.6 μM). Its derivative with a methylamine substituent, **10g** (*N*-methyl-2-(phenylsulfonyl)aniline), was ~66-times as active as diphenyl sulfone (K_i = 24.3 nM). Addition of a piperazinyl moiety in the *para*-position relative to the sulfonyl group in compound **10m** (*N*-methyl-2-(phenylsulfonyl)-5-piperazin-1-ylaniline) led to a further 150-fold increase in potency (K_i = 0.16 nM) to block the serotonin-induced response of HEK-293 cells that were stably transfected with the human recombinant 5-HT_6 receptor.

1. Introduction

The serotonin receptor of type 6 (5-HT_6R), is an attractive target for the discovery of new drugs for treatment and/or management of several CNS diseases, as evidenced by a wealth of scientific[1–5] and patent[6–8] publications. A majority of recently described 5-HT_6R antagonists contain a sulfonyl group. This class of sulfonyl 5-HT_6R antagonists can be described by four conceptual pharmacophore models, $CPhM_1$–$CPhM_4$, exemplified by the structures shown in Figure 1. These four models include common motif comprised of two hydrophobic (HYD) aromatic or heterocyclic moieties (circles), separated from each other by a hydrogen bond acceptor group (HBA), usually a sulfonyl or sulfonamide group (squares).[9–15] Either HYD moiety or both can carry substituents that provide additional interactions with the binding site.

Historically first pharmacophore model, $CPhM_3$, is exemplified by structures **1**–**3** (Fig. 1). It was suggested by Holenz et al.[9] and contains (i) two substituted HYD moieties, (ii) sulfonamide HBA group, separating the two moieties, and (iii) a highly basic positively ionisable (PI) at physiologic pH amine group, attached to either HYD moieties (filled ovals). Lopez-Rodriguez et al.[10] have further developed the pharmacophore model using a computer-aided simulation of ligand docking into a homology-based model of 5-HT_6R. Based on this model, the authors have predicted amino acid residues in the receptor binding site that could participate in the interactions with different structural features of the ligands. Later, Kim et al.[16] applied computer modeling to define a ligand pharmacophore model based on six different groups of 5-HT_6R ligands and developed the 'biggest pharmacophore model generated by a monocyclic aryl-piperazine training set', which is consistent with the $CPhM_3$ conceptual model (Fig. 1). Thus, *N*-(3,5-dichloro-2-methoxyphenyl)-4-methoxy-3-piperazin-1-ylbenzenesulfonamide **1** fits well into the 'biggest model'.[16] Out of six substituents (squares with rounded corners) encrusting both HYD moieties, 3-chloro substituent of one phenyl ring and methoxy substituent of another phenyl ring mimic the hydrophobic features of the 'biggest model', and the two phenyl HYD moieties fit within the aromatic ring zones of the model. The other highly potent 5-HT_6R antagonists of the $CPhM_3$ type are exemplified by 3-(phenylsulfonyl)-8-(piperazine-1-yl)quinoline **2** (SB-742457)[17,18] and 6-methyl-8-(piperazin-1-yl)-4-(2-chlorophenylsulfonyl)-3,4-dihydro-2H-benzo[1,4]oxazine[19] **3** (Fig. 1).

Potent 5-HT_6R ligands exemplifying the $CPhM_1$, $CPhM_2$, and $CPhM_4$ pharmacophore models are also shown in Figure 1 ($CPhM_1$: 3-(phenylsulfonyl)pyrazolo[1,5-*a*]pyrimidines **4**[20] and **5**;[21]

* Corresponding author. Tel.: +1 858 794 4860; fax: +1 858 794 4931.
E-mail address: iokun@chemdiv.com (I. Okun).

0968-0896/$ - see front matter © 2013 Elsevier Ltd. All rights reserved.
http://dx.doi.org/10.1016/j.bmc.2013.05.040

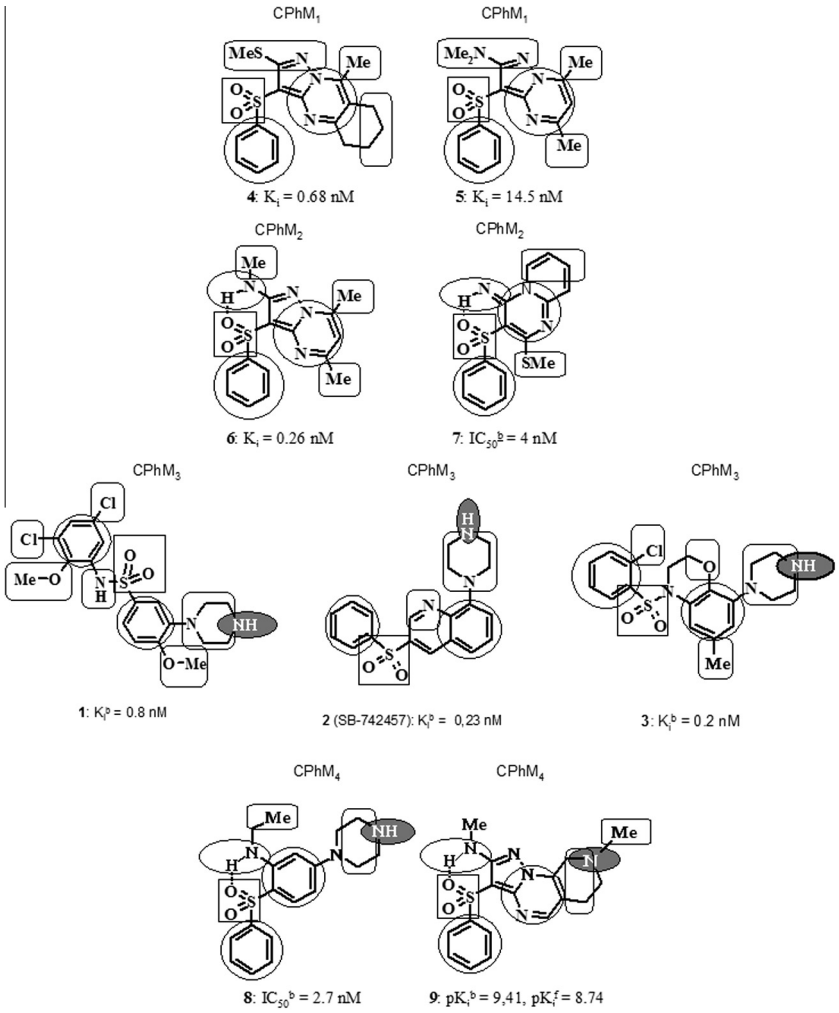

Figure 1. Conceptual pharmacophore models (intergroup distances and torsion angles are not taken into account).[9–15] Major motif is represented by two aromatic or heterocyclic hydrophobic regions, HYD (circles), separated by a sulfonyl or sulfonamide hydrogen bond acceptor group, HBA (rectangle). Additional hydrophobic substituent groups, HS (rectangles with rounded corners), can potentially interact with hydrophobic amino acids in a binding site of the 5-HT_6R. Highly basic positively ionisable group, PI (filled oval), is characteristic of models $CPhM_3$ and $CPhM_4$. Hydrogen bond donor amine, HBD (open oval) is characteristic feature of $CPhM_2$ and $CPhM_4$.

$CPhM_2$: *N*,5,7-trimethyl-3-(phenylsulfonyl)pyrazolo[1,5-*a*]pyrimidin-2-amine **6**,[21] and 2-(methylthio)-3-(phenylsulfonyl)-4*H*-pyrido[1,2-*a*]pyrimidin-4-imine) **7**;[13] $CPhM_4$: *N*-ethyl-2-(phenylsulfonyl)-5-piperazin-1-ylaniline) **8**[22] and *N*,8-dimethyl-3-(phenylsulfonyl)-6,7,8,9-tetrahydropyrazolo[1,5-*a*]pyrido[4,3-*e*] pyrimidin-2-amine) **9**[15]). Conceptual pharmacophore models $CPhM_2$ (without PI group) and $CPhM_4$ (with PI group) also contain characteristic hydrogen bond donor (HBD), amine located on one of the two HYD moieties (open ovals), which can form an intramolecular hydrogen bond with the sulphonyl HBA moiety and hence constrain the molecular conformational mobility.

Although the effects of diverse substituents on the binding affinities of different 5-HT_6R ligands are well documented, they do not seem to be universal for all chemo types. Among different structural classes of the sulfonyl-containing 5-HT_6R ligands, one can find examples in which some of the substituents are important for the binding energy in one class of ligands while being ineffective in another. Therefore, the aim of this work was to establish a validity of the above mentioned CPhMLs for the simplest ligand class, which includes diphenyl sulfone ($HYD_1 = HYD_2$ and HBA = $-SO_2-$) as a core structure. While these simplest molecules have already been considered as prospective antagonists of 5-HT_6Rs receptors,[14,23,24] their structure–activity relationship has not been studied.

To investigate the structure–activity relationship (SAR) of this class of 5-HT_6R antagonists in greater detail, we have synthesised a series of diphenyl sulfones **10**(**a**–**n**) (Fig. 2) that correspond to the above-described conceptual pharmacophore models and determined a relationship between the structural modifications, the computationally determined binding mode, and the corresponding changes in their potency to block 5-HT_6R.

2. Results and discussion

2.1. Chemistry

The synthesis of diphenyl sulfone **10a** was carried out with a yield of 83% by catalytic oxidation of diphenylsulfide in a mixture of CCl_4 and AcCN with sodium periodate in the presence of ruthenium(III) chloride hydrate, as described previously.[25]

2-(Phenylsulfonyl)aniline **10b** was obtained with a high yield using well-known methods, as outlined in reaction scheme 1 (Scheme 1). 2-Nitrodiphenyl sulfide **12** was obtained with a 99% yield by coupling 2-nitrofluorobenzene **11** and thiophenol, in accordance with previous results.[26] **12** was then oxidized by hydrogen peroxide in acetic acid[27] to yield 2-nitro-1-(phenylsulfonyl)benzene **13**, which then was reduced (as per[28]) by Fe in acetic acid to produce the desired compound **10f**. The latter was

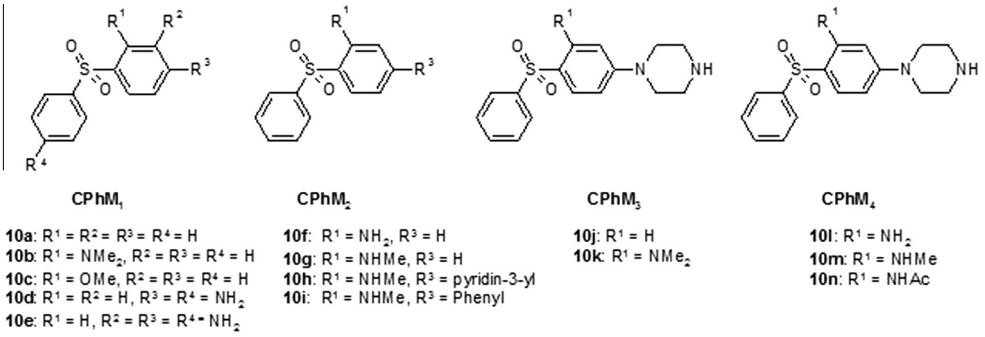

Figure 2. The synthesised diphenyl sulfones **10**(**a–n**) correspond to the discussed (Fig. 1) pharmacophore models ($CPhM_1$–$CPhM_4$) of the 5-HT_6R ligands.

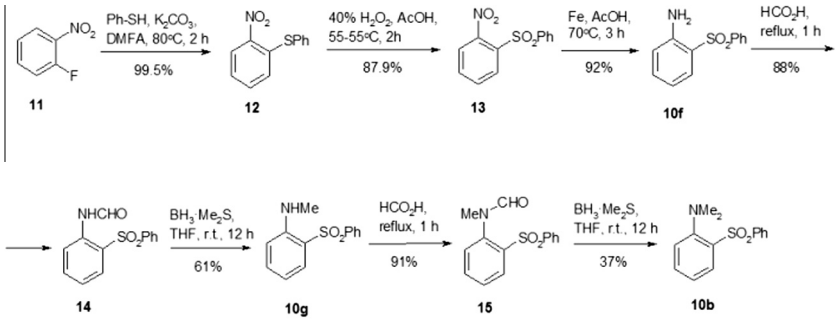

Scheme 1. Synthesis of the 2-(phenylsulfonyl)anilines **10b**, **10f** and **10g**.

converted into *N*-methyl-2-(phenylsulfonyl)aniline **10g** after formylation in accordance with[29] and subsequent reduction of the formed product **14** in THF with borane-dimethylsulfide complex. Compound **10g** was further transformed into *N*,*N*-dimethyl-2-(phenylsulfonyl)aniline **10b** by formylation and subsequent reduction of an intermediate **15**.

An X-ray analysis of **10g** (Fig. 3 and Table 1) showed that the ligand forms a dimeric structure stabilized by intra- and intermolecular hydrogen bonds.

1-Methoxy-2-(phenylsulfonyl)benzene **10c** was obtained in accordance with Scheme 2 from 1-iodo-2-methoxybenzene **16** as described previously.[30] Reaction of compound **16** with sodium phenylsulfinate in the presence of copper iodide (I) and *N*,*N*′-dimethylethylenediamine led to the target compound **10c**.

N-Methyl-2-(phenylsulfonyl)-5-(pyridin-3-yl)aniline **10h** and *N*-methyl-4-(phenylsulfonyl)biphenyl-3-amine **10i** were prepared from 1-chloro-4-iodo-2-nitrobenzene **17** in accordance with Scheme 3. Compound **17** was treated with sodium phenylsulfinate, leading to 4-iodo-2-nitro-1-(phenylsulfonyl)benzene **18**. Suzuki coupling of **18** led to 2-nitrodiphenyl sulfones **19** and **20**, which then were sequentially transformed into corresponding amines **21** and **22**, formylamines **23** and **24**, and finally, into target compounds **10h** and **10i**.

1-[4-(Phenylsulfonyl)phenyl]piperazine **10j** was obtained from 1-fluoro-4-nitrobenzene **25** in accordance with Scheme 4.

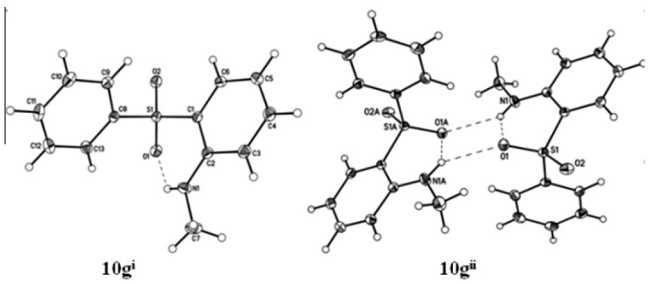

Figure 3. ORTEP of the ligand **10g** and characteristics of the intra and inter molecular hydrogen bonds.

Table 1
X-ray crystal data and structure refinement for **10g**

Identification code	**10g**
Empirical formula	$C_{13}H_{13}NO_2S$
Formula weight	247.30
Temperature	100(2) K
Wavelength	0.71073 Å
Crystal system	Monoclinic
Space group	$P2_1/n$
Unite cell dimensions	a = 8.3538(4) Å, α = 90° b = 16.9788(8) Å, β = 111.255(1)° c = 8.9309(4) Å γ = 90°
Volume	1180.57(10) $Å^3$
Z	4
Density (calculated)	1.391 Mg/m^3
Absorption coefficient	0.262 mm^{-1}
$F(000)$	520
Crystal size	0.30 × 0.20 × 0.20 mm^3
Theta range for data collection	2.40–29.99°.
Index ranges	$-11 \leqslant h \leqslant 11$, $-23 \leqslant k \leqslant 23$, $-12 \leqslant l \leqslant 12$
Reflections collected	14,794
Independent reflections	3437 [R(int) = 0.0259]
Completeness to theta = 29.99°	99.6%
Absorption correction	Semi-empirical from equivalents
Max and min transmission	0.949 and 0.925
Refinement method	Full-matrix least-squares on F2
Data/restraints/parameters	3437/0/155
Goodness-of-fit on F2	1.000
Final R indices [for 3140 rflns with $I > 2\sigma(I)$]	R_1 = 0.0316, wR_2 = 0.0803
R indices (all data)	R_1 = 0.0347, wR_2 = 0.0824
Largest diff. peak and hole	0.522 and −0.375 e $Å^{-3}$

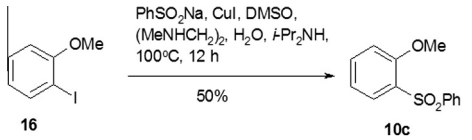

Scheme 2. Synthesis of 1-methoxy-2-(phenylsulfonyl)benzene **10c**.

Compound **25** was reacted with sodium phenylsulfinate to give 1-nitro-4-(phenylsulfonyl)benzene **26**, which was then hydrogenated to 4-(phenylsulfonyl)aniline **27** as described in.[31] Further formation of 1-iodo-4-(phenylsulfonyl)benzene **28** through diazotation followed by Buchwald–Hartwig cross coupling with piperazine in toluene in the presence of sodium *tert*-butylate and dichlorobis(tri-*o*-tolylphosphine)palladium(II) as described in,[23] resulted in compound **10j**.

Synthesis of the 2-(phenylsulfonyl)-5-(piperazin-1-yl)anilines **10**(**k**–**n**) was carried out according to Scheme 5 (Fig. 10). 5-(1-*tert*-Butoxycarbonylpiperazin-4-yl)-2-(phenylsulfonyl)aniline **29**[32] was deprotected with trifluoroacetic acid to yield 2-(phenylsulfonyl)-5-(piperazin-1-yl)aniline **10l**. *N*,*N*-Dimethyl-2-(phenylsulfonyl)-5-(piperazin-1-yl)aniline **10k** was obtained from aniline **29** by reductive alkylation, followed by removal of the Boc-group with trifluoroacetic acid. *N*-Methyl- **10m** and *N*-acetyl-2-(phenylsulfonyl)-5-(piperazin-1-yl)aniline **10n** were obtained from aniline **29** by either alkylation with dimethyl sulfate or acylation with acetic anhydride, respectively.

4,4′-Sulfonyldianiline (Dapsone) **10d** and 4-(4-aminophenylsulfonyl)benzene-1,2-diamine **10e** were obtained from a collection of ChemDiv, Inc. (USA).

The structures of the synthesised compounds were confirmed with LC–MS and NMR spectroscopy, and compound **10g** was characterized by X-ray analysis.

2.2. Computational modeling of the ligand binding to the 5-HT$_6$R

First we performed homology modeling of the human 5-HT$_6$ receptor. Currently, there are at least six GPCR proteins for which crystal structures have been solved, in some cases in complex with a ligand, with a resolution better than 3 Å: bovine rhodopsin (1HZX, resolution 2.8 Å[33] and 1U19, resolution 2.2 Å[34]); turkey β1AR with cyanopindolol (2VT4, resolution 2.7 Å); human β2AR/T4-lysozyme chimera with carazolol (2RH1, resolution 2.4 Å[35]); human D3R with eticlopride (3PBL, resolution 2.89 Å[36]); human A2AR with ZM241385 (3EML, resolution 2.6 Å[37]); and human CXCR4/lysozyme chimera with IT1t (3ODU, resolution 2.5 Å[38]). Based on sequence alignment, the highest identity score of 35% was obtained between the human 5-HT$_6$ receptor and turkey β1 adrenergic receptor with stabilising mutations (Table 2). For homology modeling of the target protein, human 5-HT$_6$R, we used two following amino acid sequences: 24–219 and 262–337; while using 3D structure of the template protein, turkey β1 adrenergic receptor, which is based on respective amino acid sequences 39–238 and 284–359.

Using the crystal structure of turkey β1 adrenergic receptor with the bound ligand cyanopindolol (PDB access code 2VT4) as a template, the 3D model of human 5-HT$_6$ receptor was built using SYBYL 8.1 (Tripos). Model loops were constructed using the LOOP Search module in SYBYL. The loop between helices 5&6 is absent in the original crystal structure; therefore, we have omitted the loop from our model structure. The model's 3D structure minimization was performed using the AMBER Force Field with Gastiger-Huckel charges (distance-dependent dielectric constant = 4.0 and nonbonded cut-off of 8 Å). Minimization was performed with a stop-gradient of 0.05 kcal/mol. An initial force field minimization was performed with the backbone atoms constrained. To reduce atomic clashes that still remained in the protein after initial minimization, 10 rounds of

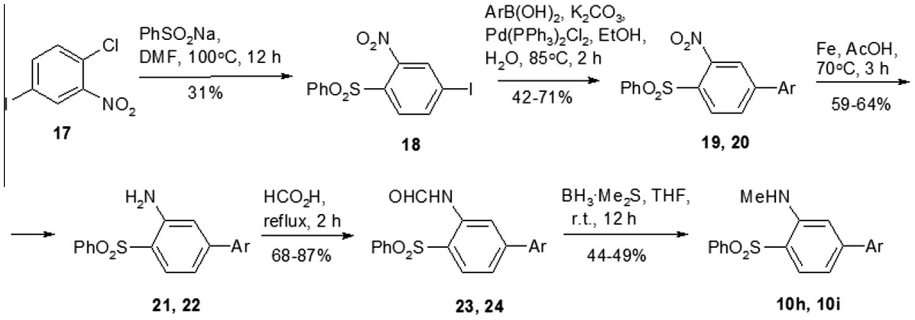

10h, 19, 21, 23: Ar = pyridin-3-yl. **10i, 20, 22, 24**: Ar = Ph.

Scheme 3. Synthesis of *N*-methyl-2-(phenylsulfonyl)-5-(pyridin-3-yl)aniline **10h** and *N*-methyl-4-(phenylsulfonyl)biphenyl-3-amine **10i**.

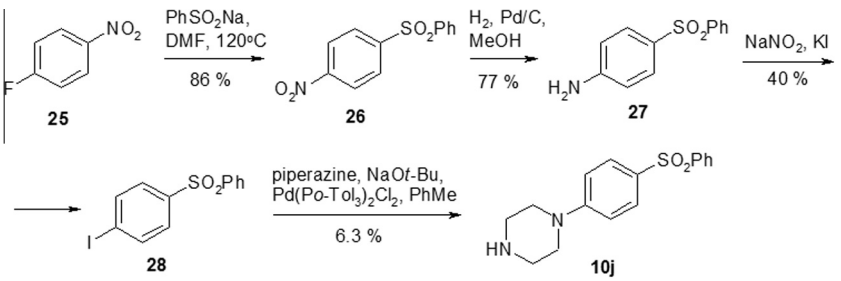

Scheme 4. Synthesis of 1-[4-(phenylsulfonyl) phenyl]piperazine **10j**.

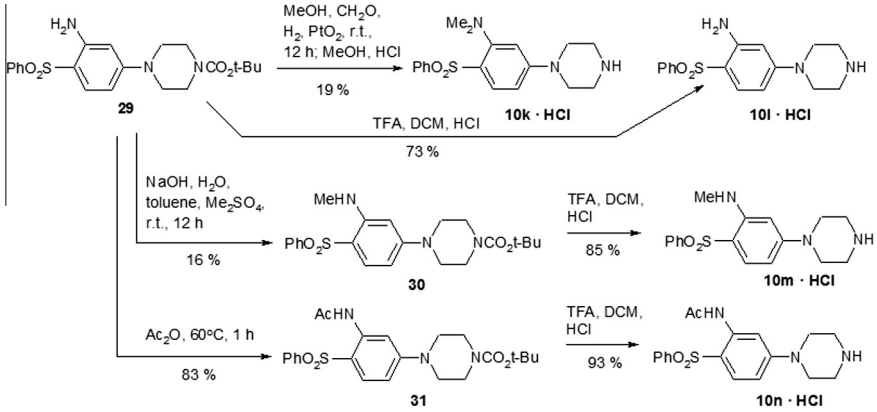

Scheme 5. Synthesis of *N*,*N*-dimethyl-2-(phenylsulfonyl)-5-(piperazine-1-yl)aniline **10k**, 2-(phenylsulfonyl)-5-(piperazine-1-yl)aniline **10l**, and its *N*-methyl- **10m** and *N*-acetyl- **10n** derivatives.

simulated annealing were performed (rise of temperature up to 600 K with subsequent annealing down to normal temperature of 200 K). After all clashes were relaxed, the final minimization was performed with all constraints removed (Table 3).

Our model seems to be structurally similar to that of Hao et al.[39] who built their 5-HT$_6$ receptor model using human β_2 AR as a template. Indeed, comparison of the turkey β_1 AR (2VT4) and human β_2 AR (2RH1) templates showed a root mean square deviation (RMSD) of 2.29 Å for Cα atoms. The RMSD between the Cα atoms of the 2VT4 structure and those in our 5-HT6R model was within resolution error at 2.74 Å.

Ligand molecules were docked in a multistep iterative process. First, using SurFlexDock (SYBYL suit), an initial positioning of the molecules was performed (after running Protoplex for a ligand preparation and Biopolimer for protein preparation), followed by subsequent docking. To explore ligand binding position, annealing was simulated by heating the complex at 600 K for 1000 fs and annealing to 200 K for 1000 fs. Finally, a three-stage restricted minimization of the ligand position was performed until either 1000 minimization steps or a field force gradient of <0.1 was achieved.

ICM-Browser Pro (MolSoft, CA) was used for visualization of the 3D structures and calculation of contact surfaces between the ligand and amino acids of the binding pocket.

2.3. Antagonistic activities of compounds 10(a–n) against 5-HT$_6$R

The functional activities of diphenyl sulfones **10**(**a–n**) as antagonists to the 5-HT$_6$R receptor were assessed in HEK-293 cells stably expressing recombinant human 5-HT$_6$ receptor.[40]

In short, activated cells expressing human recombinant 5-HT$_6$R under a tetracycline-dependent promoter were treated for 30 min with test compounds in the presence of 10 nM 5-HT (the concentration corresponding to 80–90% of maximal stimulation) and the level of intracellular cAMP was measured with a cAMP LANCE kit (PerkinElmer, USA). The concentration-dependent inhibition of 5-HT-stimulated cAMP synthesis was then fitted with a 4-parametric sigmoid equation built in Prism 5 (GraphPad, CA). The IC$_{50}$ values obtained were then converted into K_i values using Cheng-Prusoff equation.[41]

$$K_i = \frac{IC_{50}}{1 + L/K_d}$$

where K_i is the inhibition constant, IC$_{50}$ is the concentration of antagonist corresponding to a 50% blockade of the cell response to 5-HT at concentration L, and K_d is the agonist dissociation constant equivalent to the 5-HT concentration that caused half-maximal cell stimulation (EC$_{50}$). IC$_{50}$ values were determined simultaneously for each experiment by measuring cell responses as a function of 5-HT concentration. The results are shown in Table 4.

The synthesised diphenyl sulfones **10**(**a–n**) exhibited a remarkably broad (more than four orders of magnitude) range of potencies in blocking 5-HT$_6$R, ranging from K_i = 160 pM (**10m**) to K_i = 2.039 μM (**10b**). We attempted to correlate the potency values (pK_i) of the diphenyl sulfone derivatives with their general physiochemical characteristics: Log*P* (octanol/water permeation), dipole moment, partial (RPSA) and total (TPSA) polar surface areas, molecular polarisability, and radius of gyration. For this set of the diphenyl sulfone derivatives, some correlation was observed (Fig. 4) only between pK_i and molecular polarisabilities

Table 2
Sequence alignment[a] between turkey β1-adrenergic receptor and human 5HT$_6$R receptor with an alignment score of 35%. The human 5-HT$_6$ receptor sequence was obtained from www.Ebi.ac.uk SWISS-MODEL server

Protein	Amino Acid sequence	# of last amino acid
q8jg05_takru	QATASIAIAITFMMMLTIVGNILVIIAVLTSRSLKGAQNLFLVSLAAADILVATLIIPFS	60
5ht6r_human	GGSGWVAAALCVVIALTAAANSLLIALICTQPALRNTSNFFLVSLFTSDLMVGLVVMPPA	60
q8jg05_takru	LANELQGYWAFSSIWCEIYLALDVLFCTSSIVHLCAIALDRYLSISQPVSYGAKRTPVRI	120
5ht6r_human	MLNALYGRWVLARGLCLLWTAFDVMCCSASILNLCLISLDRYLLILSPLRYKLRMTPLRA	120
q8jg05_takru	KAAIIVVWMISAVISFPPLEACELNNERWYILYSTIGSFFAPCVIMILVYIRIWQIAAML	180
5ht6r_human	LALVLGAWSLAALASFLPLGQCRLLASLPFVLVASGLTFFLPSGAICFTYCRILLAAKHS	180
q8jg05_takru	NREKRFTFVLAVVMGVFVICWFPFFLSYSLQAVCPCSIPNPLFKFFFWIGYCNSCVNPVI	240
5ht6r_human	RKALKASLTLGILLGMFFVTWLPFFVANIVQAVCDCISPG-LFDVLTWLGYCNSTMNPII	239
q8jg05_takru	YTIFNNDFRKAFKRILCR	258
5ht6r_human	YPLFMRDFKRALGRFLPC	257

[a] Amino acid color code: green-polar noncharged, red-hydrophobic, blue-negatively charged and magenta-positively charged.

Table 3
Helices and loops in the 3D model of 5-HT_6 receptor

Amino acid sequence	Transmembrane domain/loop[a]
G25:C52	TM 1
T53:N59	ICL 1
T60:Y89	TM 2
G90: A95	ECL 1
R96:I128	TM 3
L129:T139	ICL 2
P140:L162	TM 4
L163:S185	ECL 2
L186:I211	TM 5
L212:S260	ICL 3
R261:A292	TM 6
V293:D295	ECL 3
C296:P321	TM 7
L322:C337	Helix 8
P338:N440	C-tail

[a] TM-transmembrane domain; ICL-intracellular loop; ECL-extracellular loop.

(R^2 = 0.36; Pearson r = 0.60; P < 0.05) and radiuses of gyration (RofG) (R^2 = 0.44; Pearson r = 0.66; P = 0.01). No significant correlation of potency to block 5-HT_6R existed with the Log$P$, dipole moment, RPSA and TPSA values. This is in compliance with our earlier findings for 5-HT_6R ligands belonging to different chemotypes.[12,21,42] We should note, however, that unlike 5,7-disubstituted *N*-methyl-3-(phenylsulfonyl)pyrazolo[1,5-*a*]pyrimidin-2-amines[42] and 3-(arylsulfonyl)pyrazolo[1,5-*a*]pyrimidines,[21] which exhibited a negative correlation between the potencies to block 5-HT_6R and the RofG, the diphenyl sulfone derivatives showed a positive correlation trend in which the compound potencies increased with molecular size.

A more detailed analysis of the apparent correlation between pK_i values and either molecular polarisabilities or RofG showed that the main component defining the apparent correlation was the presence or absence of an aryl or heterocyclic substituent in the R^3 position (the two sets of molecules are circled with dashed ovals in Fig. 4). The compounds without bulky substitution in that position (the ligands of $CPhM_1$ and $CPhM_2$ group, except for **10h** and **10i**) have generally lower polarisabilities and RofG and lower potencies than those with an aryl or heterocyclic moiety. In spite of a quite wide range of the compound potencies inside each of the two groups, with and without aryl or heterocyclic moieties, no correlation exists. For example, mono-methyl amine substitution (**10g**) in R^1 position compared to un-substituted amine in **10f** led to a 20-fold increase in potency while practically having no effect on the two physicochemical parameters. Contrary, substitution of **10g** with either pyridin-3-yl (**10h**) or phenyl (**10i**) reduced potency two-fold and six-fold, respectively, while substantially increasing polarisability and RofG. This data, in conjunction with our earlier findings, strongly indicates that attempts to correlate potencies with physicochemical characteristics of the ligands, at least for the 5-HT_6R, do not provide valid direction for designing of novel ligands.

Therefore, we have attempted to determine if observed differences in potencies upon the molecule modifications could be related to more specific interactions with the binding site of the receptor. For that, we performed molecular docking of the ligands within the 5-HT_6R binding pocket to determine if interactions between the ligands and the pocket's amino acid residues could explain the differences in their potencies.

Biphenyl sulfone **10a** (Fig. 5) is stabilized in the 5-HT_6R binding pocket through two sulfo-oxygen atoms that form three hydrogen bonds with S193(5.43) (2.13 Å), T196(5.46) (2.15 Å), and N288(6.55) (2.34 Å).

One of the phenyl rings of **10a** is immersed into a pocket formed by A184(ECL2), A192(5.42), F188(5.38), H167(ECL2), L162(4.61), L182(ECL2), V107(3.33), V189(5.39); the other phenyl ring is in contact with C110(3.36), F284(6.51), F285(6.52), as well as with V107(3.33) as the V107(3.33) is located at an equal distance from either of the two phenyl rings of **10a** and has highest contact area compared with that of other amino acids (see Table 5). Thus, besides the hydrogen bonding, the biphenyl sulfone can additionally be stabilized by hydrophobic interactions with corresponding amino acid residues in the binding pocket (Table 5).

When considering asymmetrically substituted biphenyl sulfones, energy minimization with DS Viewer Pro revealed the existence of at least two metastable conformers with substantially equal local minimum energy. The conformers differ from each other by two torsion angles, θ_A and θ_B, that describe the relative positions of the phenyl ring planes as shown in Figure 6.

Docking of **10b** (dimethylamine in R^1 position) at both stable conformations, showed a small re-orientation of the binding pose compared to **10a** (Table 5). In both conformations, conformation 1 ($\theta_A = -122.4/\theta_B = 41.5$) and conformation 2 ($\theta_A = -112.8/\theta_B = -128.9$), compound **10b** lost the hydrogen bond with N288(6.55). The loss of one hydrogen bond should have lead to a reduced binding affinity. However, a two- to three-fold increase in hydrophobic contact area with F188(5.38) or a five- to six-fold increase of the contact area with L182(ECL2) (Table 5) with the phenyl ring A (refer to Fig. 6) may essentially compensate for the loss of the hydrogen bond and thus explain the very similar potencies of **10a** and **10b**.

Docking of methoxy-substituted **10c** in either conformation (conformation 1: $\theta_A = -127.1/\theta_B = 56.3$ or conformation 2: $\theta_A = -117.3/\theta_B = -122.2$) showed that unlike the dimethylamine-substituted compound **10b**, it retained all three hydrogen bonds with the two sulfonyl oxygen atoms as was observed with **10a**. A simultaneous increase in ligand contact areas with F188(5.38) (1.5- to 2.5-fold) and L182(ECL2) (2.6- to 2.9-fold) (Table 5) could explain an increase in the antagonistic potency of **10c** relative to **10a** (Table 4).

The substitution with two amines in R^3 and R^4 positions (**10d**) leads to a 10-fold increase in the potency relative to **10a** (Table 4). Docking of the molecule into the binding pocket showed the formation of a third point of molecule coordination: the two oxygen atoms of the sulfonyl group interacting with S193(5.43) (2.13 Å) and T196(5.46) (2.14 Å), respectively, and the amino-group on either phenyl ring interacts with D106(3.32) (2.11 Å) (Fig. 7). There are no substantial changes in the amino acid contact areas except for F188(5.38) (70% increase) (Table 5). Thus, the formation of the third hydrogen bond attachment point on the molecule that coordinates and restricts the ligand mobility in the pocket could explain the increased potency.

Compared to **10d**, the addition of a third amino group in the R^2 position (**10e**) led to a ~3-fold decrease in the potency of this compound (Table 4). Analysis of the docking poses of the molecule in both conformations (conformation 1: $\theta_A = -122.8/\theta_B = 57.6$ and conformation 2: $\theta_A = -122.8/\theta_B = -122.6$) did not conclusively explain the unexpected three-fold decrease in the potency. Indeed, **10e** maintains the same three points of attachment through hydrogen bonds: the first two consist of one sulfonyl oxygen atom bonding with S193(5.43) (2.13 and 2.15 Å) and the other sulfonyl oxygen atom bonding with T196(5.46) (2.14 and 2.21 Å); the third is the bond between the amino-group on the phenyl ring B and D106(3.32) (2.11 Å in both conformations). Calculations of the contact surface areas did not show any substantial decrease in nonpolar interactions. In contrast, the contact area of L182(ECL2) showed a two-fold increase for the first ligand conformation and a three-fold increase for the second ligand conformation. One plausible explanation of the lower potency of **10e** relative to **10d** is a

Table 4
5-HT_6R antagonistic potency of substituted diphenyl sulfones **10**(**a**–**n**)

Pharmac. model	Cpd ID 10	R Group substitutions (refer to Fig. 2)				K_i (nM)	Rel. pot.[a]
		R^1	R^2	R^3	R^4		
$CPhM_1$	a	H	H	H	H	1598	1
$CPhM_1$	b	NMe_2	H	H	H	2039	0.80
$CPhM_1$	c	OMe	H	H	H	866	1.80
$CPhM_1$	d	H	H	NH_2	NH_2	183	8.73
$CPhM_1$	e	H	NH_2	NH_2	NH_2	564	2.83
$CPhM_2$	f	NH_2		H		491	3.25
$CPhM_2$	g	NHMe		H		24.3	65.80
$CPhM_2$	h	NHMe		Pyridin-3-yl		48.3	33.08
$CPhM_2$	i	NHMe		Ph		153	10.50
$CPhM_3$	j	H				10.8	148
$CPhM_3$	k[b]	NMe_2				30.1	53.10
$CPhM_4$	l	NH_2				1.65	968.50
$CPhM_4$	m	NHMe				0.16	9987.50
$CPhM_4$	n	NHAc				8.3	192.50

[a] Relative potency is calculated as a ratio of the K_i of **10a** to that of the given compound.
[b] Compound exhibits partial agonism (17% activation without 5-HT present in the solution).

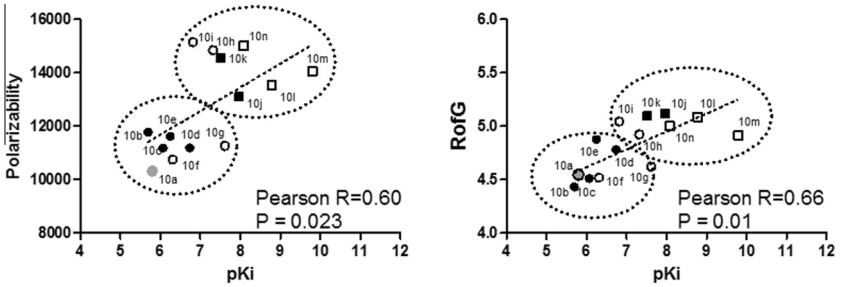

Figure 4. Correlation between compound potencies (pK_i) and their physiochemical characteristics as calculated in DS Viewer Pro 6.0 (Accelris). The average values for Radius of gyration (RofG) ± SD are calculated for several local minima conformations of the molecules. Grey circle-diphenyl sulfone; closed circles-compounds of $CPhM_1$; open circles-compounds of $CPhM_2$; closed squares-compounds of $CPhM_3$; and open squares-compounds of $CPhM_4$.

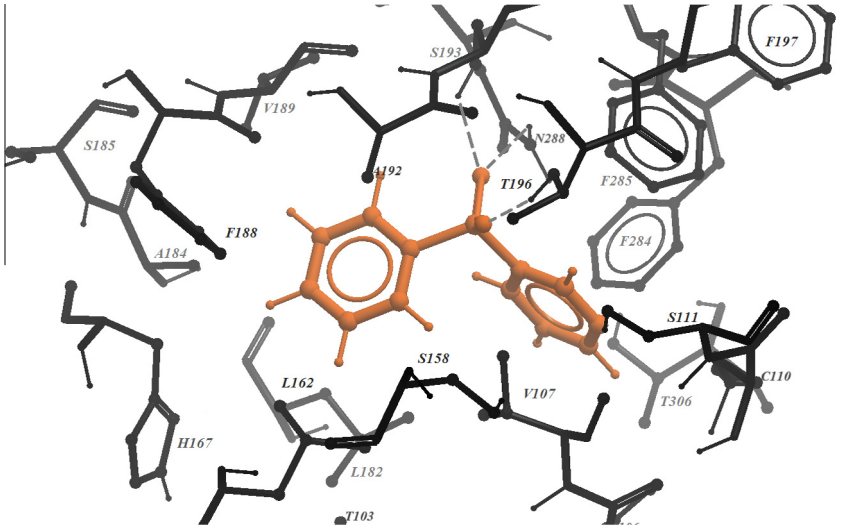

Figure 5. The binding mode of **10a** (brown) into the 5-HT_6R model. Amino acid residues in black are located in front of the **10a** molecule and those in gray-behind it. Gray dashed lines represent hydrogen bonds between sulfo oxygen atoms of **10a** and amino acid residues S193(5.43) and T196(5.46) of helix five and N288(6.55) of helix six.

desolvation energy penalty incurred as the highly polar R^2 amino-group approaches the nonpolar environment provided by either L182(ECL2) or C110(3.36), depending on the molecular conformation docked. Contact areas of all other amino acids with **10e** in either conformation are similar to those of **10d** (Table 5).

Energy minimization of the compounds in the $CPhM_2$ series (**10f–i**) showed that these compounds have two deep local free energy minima; their intramolecular conformational mobility is characteristically restricted through the formation of an intramolecular hydrogen bond between either of the sulfonyl oxygen atoms and

Table 5
Contact areas of amino acid residues located in a vicinity of the ligand molecules as calculated using ICM browser

Model	**Cpd ID**[a] (θ_A/θ_B)	**Phenyl A** (Fig. 6)										**Sulfonyl**[b]			**Ph B + R3** (Fig. 6)					
		A184	A192	F188	H167	L162	L182	S158	T103	V107	V189	N288	S193 (Å)	T196 (Å)	D106	T306	Y310	G309	W102	W281
$CPhM_1$	**10a**	10.0	18.8	3.8	6.0	14.5	3.1		0.6	38.4	16.1	**2.34 Å**	**2.13**	**2.15**	6.2					
	10b-C1 (−122.4/41.5)	8.5	20.1	7.7	6.0	14.2	19.2			36.8	16.5	17.2	**2.14**	**2.19**	6.8					
	10b-C2 (−112.8/−128.9)	1.6	20.1	12.0	2.5	13.5	17.3			36.2	15.1	19.2	**2.13**	**2.34**	5.6	1.0				
	10c-C1 (127.1/56.3)	9.1	19.2	5.6	6.6	14.5	8.2			37.1	15.6	**2.38 Å**	**2.12**	**2.16**	3.9					
	10c-C2 (−117.3/−122.2)	7.5	18.8	9.3	4.7	14.2	9.1			37.4	15.4	**2.47 Å**	**2.13**	**2.26**	2.5	1.0				
	10d	9.4	21.4	6.4	6.3	14.5	3.4			35.6	17.6	17.1	**2.13**	**2.14**	**2.11 Å**[c]	3.5				
	10e-C1 (−122.8/57.6)	9.4	21.0	7.2	5.8	13.8	10. 7			36.5	17.6	18.1	**2.13**	**2.14**	**2.11 Å**[c]	4.1				
	10e-C2 −122.8/−122.6)	8.8	19.5	10.5	5.5	14.5	7.5			35.9	16.9	17.6	**2.15**	**2.21**	**2.11 Å**[c]	5.4	0.6			
$CPhM_2$	**10f**-C1 (−132.3/61.8)	9.4	18.5	5.5	6.3	14.2	2.8			37.1	15.8	**2.46 Å**	**1.14**	**2.18**	5.0					
	10f-C2 (−123.8/−126.8)	9.7	20.1	4.7	6.6	13.8	2.5			41.6	16.8	**2.35 Å**	**2.13**	**2.14**	5.1					
	10g-C1 (128.1/61.0)	8.5	19.4	6.6	6.6	16.0	10.0		0.3	37.8	15.6	**2.45 Å**	**2.12**	**2.16**	4.2					
	10g-C2 (−121.8/−117.3)	7.8	18.5	9.4	5.3	14.2	10.7			36.2	15.6	**2.5 Å**	**2.12**	**2.28**	1.0	1.0				
	10h-C1 (−105.4/+91.6)	9.1	19.2		1.9	11.3	3.2		1.2	35.6	11.5	25.0	**2.11**	**2.11**	11.4	17.1	13.0	11.4		
	10h-C2 (−119.3/−117.7)	6.6	22.0	3.2	2.5	14.8				38.5	12.0	21.4	**2.11**	**2.16/2.28**[d]	11.3	12.5	13.9	9.9		1.2
	10i-C1 (−105.4/91.6)	9.4	18.5		1.9	11.3	3.2		1.2	36.5	10.9	25.6	**2.11**	**2.10**	11.3	17.6	14.0	11.8		
	10i-C2 (−122.4/−121.0)	5.01	22.6	12.6	6.6	16.7		2.2		40.5	13.9	14.3	**2.13**	**2.21/2.33**[d]	13.2	14.4	12.2	4.9		
$CPhM_3$	**10j**	8.5	21.3	10.2	5.3	16.4	15.1			34.0	16.1	**2.46 Å**	**2.11**	**2.19**	**2.15 Å**[e]	26.2	**2.31 Å**[e]		5.3	
	10k-C1 (−126.0/49.5)	14.1	18.2	11.4	5.0	16.0	28.9			33.0	21.7	16.0	**2.11**	**2.23**	**2.22 Å**[e]	25.6			5.3	
	10k-C2 (−120.4/−120.0)		19.2	15.0	1.6	12.9	33.0			32.7	14.0	20.9	**2.14**	**2.37**	16.2	**1.97 Å**[e]	4.5		15.7	
$CPhM_4$	**10l**-C1 (−129.5/60.8)	8.2	19.8	10.5	5.6	17.0	12.6		0.6	34.6	15.4	15.6	**2.11**	**2.20**	**2.17 Å**[e]	25.3	14.1		2.2	
	10l-C2 (−119.6/−125.6)	8.8	18.2	9.3	5.6	16.7	17.3			34.9	15.5	**2.47 Å**	**2.12**	**2.19**	**1.84 Å**[e]	26.6	**2.42 Å**[e]		7.8	
	10m-C1 (−128.7/56.4)	8.2	19.4	10.2	6.0	16.7	21.0		0.6	34.3	18.4	2.64 **Å**	**2.11**	**2.20**	**2.14 Å**[e]	25.3	13.2		3.1	
	10m-C2 (−122.6/−119.5)	6.9	18.5	10.2	5.0	16.3	21.7			36.8	15.8	**2.5 Å**	**2.12**	**2.26**	**2.07 Å**[e]	24.3	**2.26 Å**[e]		11.6	
	10n-C1 (−129.3/57.4)	12.6	19.4	10.2	6.3	16.4	22.0		0.6	34.3	26.2	19.5	**2.11**	**2.20**	**2.15 Å**[e]	27.1	13.2		0.9	
	10n-C2 (−121.0/−117.2)	9.1	18.2	9.6	6.0	16.0	21.7			41.2	14.9	**2.47 Å**	**2.11**	**2.25**	**2.02 Å**[e]	22.1	**2.41 Å**[e]		11.6	

[a] C1 and C2 relate to a particular semi-stable conformations found in a docking procedure with characteristic torsion angles shown in parentheses (refer to Fig. 6).
[b] Hydrogen bonds formed with sulfonyl oxygen atoms are shown in bold as the length between oxygen and a proton of a corresponding amino acid residue group forming the bond.
[c] Hydrogen bonds formed with *p*-NH_2 of the phenyl ring B are shown in bold as the length between oxygen and a proton of a corresponding amino acid residue group forming the bond.
[d] Hydrogen bonds formed with *o*-$NHCH_3$ of the phenyl ring B are shown in bold as the length between oxygen and a proton of a corresponding amino acid residue group forming the bond.
[e] Hydrogen bonds formed with the secondary amine of the piperazine moiety are shown in bold as the length between oxygen and a proton of a corresponding amino acid residue group forming the bond.

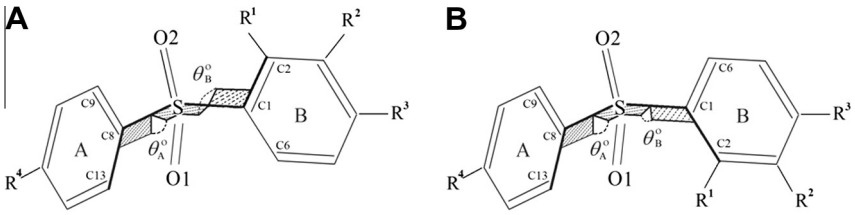

Figure 6. A schematic representation of the two most stable configurations for asymmetric biphenyl sulfones with torsion angles θ_A and θ_B. The bonds used in calculating the torsion angles are shown with bold lines.

the amino or methylamino group. An example based on compound **10g**, for which the X-ray structure has been determined, is shown in Figure 8.

The X-ray structure of **10g** (Fig. 3) showed that the distance between one of the oxygen atoms and the nitrogen atom is compatible with the formation of the intramolecular hydrogen bond and is very similar to the distances observed in docked conformations.

On average, the potency to block 5-HT$_6$R is an order of magnitude higher for compounds in the CPhM$_2$ series than that of compounds in the CPhM$_1$ series (Fig. 9). Thus, substituting the dimethylamine of **10b** (which does not form the intramolecular hydrogen bond) with an amine group, as in **10f**, led to a 4-fold increase in the antagonistic potency of the compound (Table 4). Depending on the conformation chosen for the docking, **10f** is stabilized either by three or by two coordination points. In one conformation, two sulfo-oxygen atoms form hydrogen bonds with S193(5.43) and T196(5.46), respectively, and amino substituent group forms the third hydrogen bond with oxygen of N288(6.55). In second conformation, two hydrogen bonds are formed between one oxygen atom with S193(5.43) and N288(6.55) and the third hydrogen bond is formed between other sulfonyl oxygen atom and T196(5.46). In both cases, the amino group of **10f** maintains the intramolecular mobility-restricting hydrogen bond with either sulfonyl oxygen atom.

Substituting an amino group in the R^1 position of **10f** with a methylamino group (**10g**) leads to an additional 20-fold increase in the compound's potency (Table 4). Molecular docking of the **10g** in either stable conformation (conformation 1: $\theta_A = -128.1/\theta_B = 61.0$; and conformation 2: $\theta_A = -121.8/\theta_B = -117.3$) suggests that both conformations can be accommodated into the binding site of the receptor with two pose-restricting 'points of attachment': one sulfonyl oxygen atom forms two hydrogen bonds with S193(5.43) and N288(6.55) and the other oxygen atom bonds with T196(5.46). In each of the two conformations, the methyl amino group of **10g** maintains the intramolecular conformation mobility-restricting hydrogen bond with either of the sulfonyl oxygen atoms. The binding pose could also explain the additional binding energy of **10g** relative to **10f** through forming additional hydrophobic interactions of the methyl residue of the methylamino group with the receptor binding site amino acid residues. Indeed, in conformation 1, the methyl of the methylamine group is directed towards the hydrophobic amino acid residues F284(6.51) and L182(ECL2). In conformation 2, the methyl group is in close van Der Waals contact proximity with the hydrophobic residues V107(3.33), C110(3.36), and F285(6.52), and unfavourable contact between the hydrophobic phenyl B ring and the highly hydrophilic D106(3.32) residue is reduced (Table 5).

Modification of the methylamino-substituted **10g** by addition of either pyridin-3-yl (**10h**) or phenyl (**10i**) into the R^3 position leads, respectively, to two-fold and 6.3-fold decreases in the antagonistic potency relative to **10g**. This potency decrease could be a result of reduced number of hydrogen bonds in one of the two stable conformations in both molecules (Table 5). Indeed, conformations **10h**-C1 and **10i**-C1 are stabilized by only two hydrogen bonds between the sulfo-oxigen atoms and S193(5.43) and T196(5.46), respectively. In another conformation, the molecules do form additional hydrogen bond between oxygen of the same T196(5.46) residue and methylamine moiety of either molecule. Besides, the phenyl ring in **10i** comes into an unfavorable hydrophobic/hydrophilic proximity to the highly polar D106(3.32), which could also contribute to the lower potency of **10i** comparative to **10h** (Table 4). However, when **10g** is substituted with a piperazin-1-yl moiety

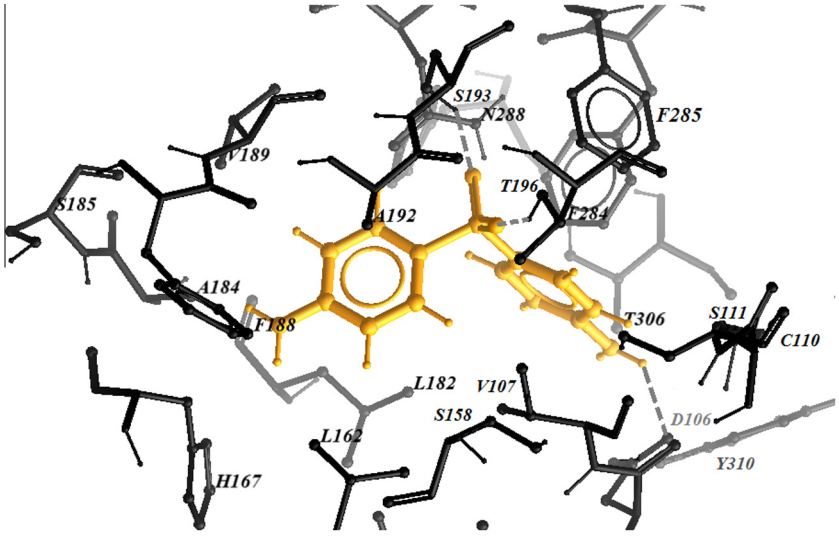

Figure 7. The binding mode of **10d** in the 5-HT$_6$R model. Coloring scheme of the amino acid residues in the binding pocket is the same as in Fig. 6.

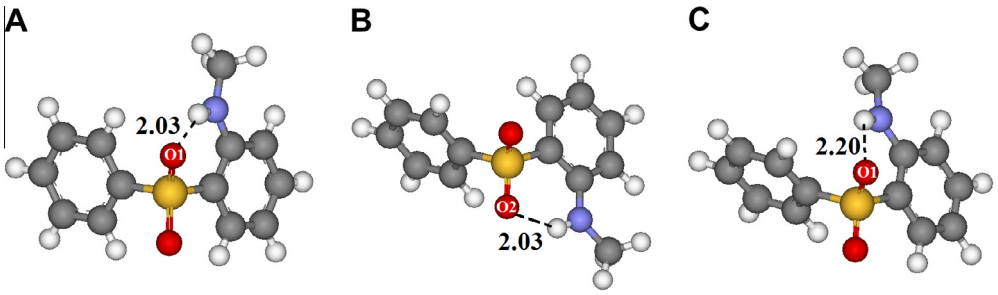

Figure 8. Structures of **10g** obtained from X-ray experiments (A); and its two docked, stable conformations extracted from the receptor-ligand complexes (B and C). The distances between atoms are in angstroms.

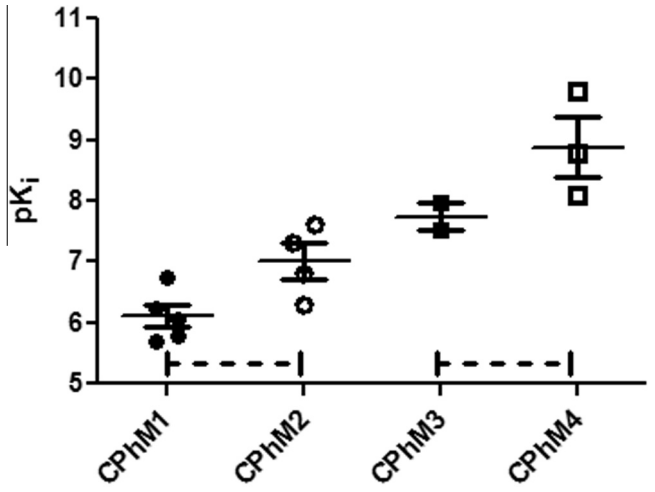

Figure 9. Potencies (pK_i) of the diphenyl sulfones belonging to different conceptual pharmacophore models.

(**10m**, $CPhM_4$) instead of a phenyl or pyridin-3-yl moiety, the antagonistic potency to block 5-HT_6R jumps 150-folds (from K_i = 24.3–0.16 nM) (Table 4). Similar to the compounds of the $CPhM_2$ series, **10m** has a hydrogen bond that restricts intramolecular conformational mobility (Fig. 2). Docking of **10m** into 5-HT_6R revealed that besides two hydrogen bond-forming sulfonyl oxygen atoms, a secondary amine in the piperazin-1-yl provides third coordination point through formation of either a hydrogen bond or a salt bridge with D106(3.32). In the conformation C2 (Table 5), the **10m** is stabilized in the binding pocket by at least five hydrogen bonds: three bonds between residues S193(5.43), T196(5.46), and N288(6.55) and two sulfo-oxygen atoms and two bonds (one of them could be a salt bridge) between D106(3.32) and Y310(7.43).

In the $CPhM_3$ and $CPhM_4$ compound series, presence of the piperazine-1-yl moiety at R^3 generally leads to a substantial increase in potency. Thus, 1-(4-(phenylsulfonyl)phenyl)-piperazine **10j** exhibits a 150-fold greater potency than its nonsubstituted analogue, diphenyl sulfonyl (**10a**). In spite of its ability to be positively ionized, substitution with a dimethylamino group in position R^1 (**10k**) leads to a three-fold decrease in the antagonistic potency compared to **10j**. This is consistent with the slight decrease in potency upon analogous substitution in the $CPhM_1$ series (compare **10b** with **10a**, Table 4). On the other hand, when the R^1 position is substituted with an amine (**10l**) or methylamine (**10m**) moieties that can form intramolecular hydrogen bonds, respectively, 6.5-fold and 67.5-fold potency increases are observed relative to the unsubstituted analogue **10j** (Table 4). Acetyl amino substitution in the R^1 position of **10n** did not change the potency (K_i = 8.3 nM) compared to that of the unsubstituted and structurally unrestricted analogue **10j** (K_i = 10.8 nM). Meanwhile, the acetyl amine in **10n** can also form an intramolecular hydrogen bond with the sulfonyl oxygen atoms, which yields two metastable conformations (conformation 1: $\theta_A = -126.5/\theta_B = 56.4$; and conformation 2: $\theta_A = -114.5/\theta_B = -114.4$). We attempted to see if the docking of **10n** into the 5-HT_6R model could shed some light on the reason behind the absence of the potency increase of **10n** in spite of being conformationally restricted, as compared with unrestricted **10j**. Indeed, the binding pose of **10n** revealed that the acetyl oxygen is located in an unfavorable proximity with the nonpolar amino acid residues: in conformation 1 with L182(ECL2) or, in conformation 2, with V107(3.33), F285(6.52), and C110(3.36). The compounds in the $CPhM_2$ and $CPhM_4$ series have conformational mobility restrictions afforded by intramolecular hydrogen bonds and in general exhibit higher potencies than their corresponding unrestricted analogues from series $CPhM_1$ and $CPhM_3$ (Fig. 9).

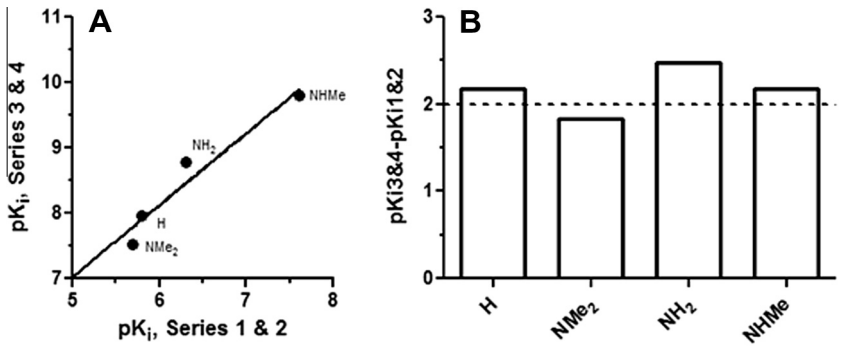

Figure 10. A. Correlation between 5-HT_6R antagonistic potencies (pK_i) of the compounds with R^3 = H (series 1 and 2) and those with piperazine-1-yl substitution at R^3 position (series 3 and 4). The labels show R^1 substituent group. **B.** Difference in potencies between identical substitutions in R^1 position in corresponding pares of series 1 and 2 (R^3 = H) and piperazin-1-yl-containing series 3 and 4.

The unfavorable immersion of the acetyl oxygen of **10n** into nonpolar microenvironment could negatively compensate for the gain in potency attributed to the intramolecular mobility restriction.

An analysis of the influence of R^1 substitution on the ability of compounds to block 5-HT_6Rs in series with R^3 = H and R^3 = piperazin-1-yl-substitutions, shows that the R^1 substitutions have practically identical effect in both series (Fig. 10). Indeed, when plotting potency values of compounds in one series as a function of identically R^1 substituted compounds in the other series, a fair linear dependence (R^2 = 0.94) with a slope equal to unity (1.1 ± 0.2) is observed (Fig. 10A). There is a difference of approximately two orders of magnitude in potency between compounds with identical R_1 groups belonging to the $CPhM_1$ and $CPhM_2$ series (R^3=H) and those of the $CPhM_3$ and $CPhM_4$ series (piperazin-1-yl-substitution at R^3 position) (Fig. 10B). Thus, the substitution of either biphenyl sulfone or 1-(4-(phenylsulfonyl)phenyl)piperazine in the R^1 position with a primary amine or a secondary methylamine provides a two orders of magnitude potency improvement range in both series. This agrees well with our previous observations that conformational restriction of a ligand molecule with intramolecular hydrogen bond has a positive effect on potency against 5-HT_6R in the following series of compounds: 3-(arylsulfonyl)pyrazolo[1,5-*a*]pyrimidines,[21] 3-(phenylsulfonyl)pyrazolo[1,5-*a*]pyrido[3,4-*e*]pyrimidines and 3-(phenylsulfonyl)pyrazolo[1,5-*a*]pyrido[4,3-*d*]pyrimidines;[43] and 3-(phenylsulfonyl)cycloalkano[*e* and *d*]pyrazolo[1,5-*a*]pyrimidin-2-amines.[44]

Formation of the third coordinating centre between piperazin-1-yl of the ligand and D106(3.32) (in one of the two metastable conformations) or with both the D106(3.32) and Y310(7.43) (for the other metastable conformation) is characteristic of the piperazin-1-yl substituted series. This adds an additional two orders of magnitude to the increase in potency of all molecules with similar R^1 substitutions.

3. Conclusions

Synthesised derivatives of diphenyl sulfones are the smallest and simplest ligands to show quite impressive potency in blocking serotonin-induced responses in HEK293 cells stably transfected with recombinant human 5-HT_6 receptor. In conjunction with our previous data, the QSAR analyses of observed changes in the potencies of the diphenyl sulfones in relation with different quantitative physiochemical parameters did not produce reliable means that would allow for targeted design of potent 5-HT6R ligands. In this respect, molecular docking into a 3D model of the 5-HT_6 receptor modeled after turkey β1-adrenoreceptor crystal structure, allowed us to suggest binding poses of the synthesized ligands that could reasonably explain observed changes in compound potencies upon specific substitutions. In accordance with our model, S193(5.43) and T196(5.46) and, in some cases, N288(6.55) form hydrogen bonds with two oxygen atoms of the ligands sulfonyl moiety. This can potentially explain quite high antagonist potency of the simplest biphenyl sulfone. Addition of a primary or secondary amine substituent in R^1 position restricts intramolecular conformation mobility through formation of an intramolecular hydrogen bond with one of the sulfonyl oxygen atoms, thus substantially increasing compound potencies. However, the nature of the amine substitution (methyl, methoxy, or acetyl) substantially affects the potency. Substitution of the diphenyl sulfone and its derivatives with pipeazin-1-yl in the *para* position to the sulfonyl group adds an additional two orders of magnitude in potency, which can be attributed to generation of a third coordination point by formation of either a hydrogen bond or a salt bridge between the pipeazin-1-yl nitrogen and D106(3.32).

Asymmetric molecules (especially those with intramolecular mobility restrictions) can exist in several metastable conformations. It is not obvious which conformations, or if all conformations, of a ligand can be accommodated in the binding pocket. Therefore, energy minimization of the binding pose should be performed by starting annealing process with alternate ligand conformations and analyzing the contacts that the ligand makes in different poses with the amino acid residues in a binding pocket.

Though the modeling of binding pose of diphenyl sulfones does not provide direct proof of the amino acid residues involved into the binding, it gives a direction on what additional features could be explored in the ligand design to further increase its affinity and, hopefully, selectivity. Further confirmation of the particular amino acid residues predicted to be involved in the binding of this class of ligands will be considered in direct mutagenesis experiments.

4. Experimental section

Starting materials were either commercially available or purchased from Sigma–Aldrich (St Louis, MO, USA). Solvents and reagents were used without further purification unless otherwise specified. ^{1}H NMR spectra were recorded on Bruker DPX-400 (400 M Γ ιι, 27 °C) instruments in DMSO-d_6 or $CDCl_3$. Chemical shifts (δ) are reported in ppm downfield from an internal TMS standard.

LC–MS data were obtained using a Shimadzu HPLC equipped with a Waters XBridge C_{18} 3.5 mm column (4.6 × 150 mm), PE SCIEX API 150 EX mass detector, and Shimadzu spectrophotometric detector (λ, 220 and 254 nm). In all cases, the completion of the reaction was determined by conversion of the substrate (LC–MS control).

Reaction product separation was performed using an HPLC system with Shimadzu LC-8A on the chromatographic column Reprosil-Pur C-18-AQ 10, 250 × 20 mm (pre-column Reprosil-Pur C-18-AQ 10, 50 × 20 mm) at a flow rate of 25 mL/min in gradient mode with mobile phase MeCN/water +0.05% CF_3COOH.

X-ray analysis: data collection: SMART (Bruker, 1998); cell refinement: SAINTPlus (Bruker, 1998); data reduction: SAINTPlus (Bruker, 1998); program(s) used to solve structure: SHELXTL ver. 5.1 (Sheldrick, 1998); program(s) used to refine structure: SHELXTL ver. 5.1 (Sheldrick, 1998); molecular graphics: SHELXTL ver. 5.1 (Sheldrick, 1998); software used to prepare material for publication: SHELXTL ver. 5.1 (Sheldrick, 1998).

4.1. Procedures for synthesis of compounds 10a–n

Diphenyl sulfone **10a** was obtained according to.[25] LS MC *m*/*z* 219 (M+1). ^{1}H NMR (DMSO-d_6, 400 MHz) δ 7.95 (d, *J* = 7.6 Hz, 4H), 7.69 (t, *J* = 7.2 Hz, 2H), 7.618 (t, *J* = 7.6 Hz, 4H).

4,4′-Sulfonyldianiline (Dapsone), **10d**, and 4-(4-aminophenylsulfonyl)benzene-1,2-diamine, **10e**, were obtained from ChemDiv, Inc. (USA).

1-(4-(Phenylsulfonyl)phenyl)piperazine **10j** was obtained as described previously.[45] LS MC *m*/*z* 303 (M+1). ^{1}H NMR ($CDCl_3$, 400 MHz) δ 7.87 (m, 2H), 7.85 (m, 2H), 7.51 (m, 3H), 6.94 (m, 3H), 3.58 (m, 4H), 3.33 (m, 4H), 2.18 (m, 1H).

N,*N*-Dimethyl-2-(phenylsulfonyl)aniline **10b**. A solution of 200 mg (0.81 mmol) of *N*-methyl-2-(phenylsulfonyl)aniline **10g** in 5 mL of formic acid was refluxed for 1 h. The cooled mixture was roto-evaporated, dissolved in chloroform, washed with a saturated $NaHCO_3$ solution and washed with water. The organic layer was dried over Na_2SO_4 and roto-evaporated. The crude product was purified by column chromatography (eluent-hexane/AcOEt 4:1) to afford 205 mg (92%) of *N*-methyl-*N*-(2-(phenylsulfonyl)phenyl)formamide **15**. A solution of a borane dimethyl sulfide complex (2 M in THF, 1.1 mL, 2.19 mmol) was added to a solution

of 200 mg (0.73 mmol) of compound **15** in 5 mL of THF, and the mixture was stirred at ambient temperature for 12 h under Ar. The solution was quenched with a saturated $NaHCO_3$ solution and extracted with DCM. The extract was dried over Na_2SO_4 and roto-evaporated. The crude product was purified by HPLC to afford 70 mg (37%) of **10b**. LS MC *m*/*z* 262 (M+1). ^{1}H NMR (DMSO-d_6, 400 MHz) δ 8.10 (dd, J_1 = 7.6 Hz, J_2 = 0.8 Hz, 1H), 7.79 (d, J = 7.6 Hz, 2H), 7.69 (m, 1H), 7.64 (t, J = 7.2 Hz, 1H), 7.55 (t, J = 7.6 Hz, 2H), 7.45 (d, J = 7.6 Hz, 1H), 7.42 (d, J = 7.6 Hz, 1H), 2.31 (s, 6H).

1-Methoxy-2-(phenylsulfonyl)benzene **10c**. A mixture of 144 mL (1 mmol) of 85% *N*,*N*′-dimethylethylenediamine and 96 mg (0.5 mmol) of CuI in 7 mL of DMSO was stirred for 5 min to dissolve CuI. Then, 2.7 mL of water, 0.87 mL (5 mmol) of DIPEA, 1.64 g (10 mmol) of sodium phenylsulfinate and 1.17 g (5 mmol) of 1-iodo-2-methoxybenzene **16** (obtained according to[29]) were successively added. The mixture was stirred under argon at 100 °C for 12 h and then cooled down and stirred at ambient temperature for 5 h. The mixture was filtered, treated with water and extracted with DCM. The extract was washed with water, dried over Na_2SO_4 and roto-evaporated. The crude product was purified by column chromatography (eluent-hexane/AcOEt 4:1) to afford 1.26 g (50%) of **10c**. LS MC *m*/*z* 249 (M+1). ^{1}H NMR (DMSO-d_6, 400 MHz) δ 8.00 (d, J = 7.6 Hz, 1H), 7.88 (d, J = 7.6 Hz, 2H), 7.67 (m, 2H), 7.59 (t, J = 6.8 Hz, 2H), 7.19 (d, J = 7.6 Hz, 1H), 7.15 (d, J = 8 Hz, 1H), 3.72 (s, 3H).

2-(Phenylsulfonyl)aniline **10f**. A 5.22 g (0.09315 mol) aliquot of iron (powder) was added gradually to a suspension of 4.9 g (0.01863 mol) of 2-nitrodiphenylsulfone **11**, obtained according to previous results,[26,27] in 60 mL of acetic acid. The mixture was stirred for 3 h at 70 °C, cooled and filtered from inorganic impurities. A 100 mL aliquot of water was added to the obtained solution. The formed precipitate was filtered, washed with water and dried in vacuum. The yield of **10f** was 4 g (92%). LS MC *m*/*z* 234 (M+1). ^{1}H NMR (DMSO-d_6, 400 MHz) δ 7.91 (d, J = 8 Hz, 2H), 7.67 (t, J = 9.6 Hz, 2H), 7.58 (t, J = 7,6 Hz, 2H), 7.29 (t, J = 7.2 Hz, 1H), 6.77 (d, J = 8.4 Hz, 1H), 6.67 (t, J = 7.6 Hz, 1H), 6.12 (s, 2H).

N-Methyl-2-(phenylsulfonyl)aniline **10g**. A solution of borane dimethyl sulfide complex (2 M in THF, 2.65 mL, 5.28 mmol) was added to a solution of 460 mg (1.76 mmol) of *N*-formyl-2-(phenylsulfonyl)aniline **14** in 11 mL of THF. The mixture was stirred at ambient temperature for 12 h under Ar. The solution was quenched with saturated $NaHCO_3$, extracted with DCM, and then the extract was dried over Na_2SO_4 and roto-evaporated. The crude product was purified by column chromatography (eluent-hexane/AcOEt 4:1) and recrystallized from AcOEt to afford 264 mg (61%) of **10g**. LS MS *m*/*z* 248 (M+1). ^{1}H NMR (DMSO-d_6, 400 MHz) δ 7.95 (d, J = 7.2 Hz, 2H), 7.78 (dd, J_1 = 9.6 Hz, J_2 = 1.2 Hz, 1H), 7.66 (t, J = 7,6 Hz, 1H), 7.58 (t, J = 7.6 Hz, 2H), 7.44 (t, J = 8 Hz, 1H), 6.75 (d, J = 7.2 Hz, 1H), 6.71 (d, J = 8 Hz, 1H), 2.79 (d, J = 4.8 Hz, 3H).

N-Methyl-2-(phenylsulfonyl)-5-(pyridin-3-yl)aniline **10h**. A mixture of 4.9 g (17.4 mmol) of 1-chloro-4-iodo-2-nitrobenzene **17** and 2.85 g (17.4 mmol) of sodium phenylsulfinate in 70 mL of DMF was stirred at 120 °C for 12 h. The mixture was cooled down, diluted with water and extracted with AcOEt. The extract was dried over Na_2SO_4 and roto-evaporated. Purification by column chromatography (eluent – hexane/AcOEt 4:1) afforded 2.07 g (31%) of 4-iodo-2-nitro-1-(phenylsulfonyl)benzene **31**. A mixture of 110 mg (0.9 mmol) of pyridin-3-ylboronic acid and 240 mg (2.26 mmol) of Na_2CO_3 in 8.8 mL of ethanol and 2.2 mL of water was stirred at 90 °C under Ar for 40 min and then cooled down. To this mixture, 432 mg (1.12 mmol) of compound **18** was added, followed by 20 mg of $Pd(PPh_3)_2Cl_2$. The mixture was stirred at 85 °C under Ar for 2 h and then cooled, diluted with water and extracted with DCM. The extract was washed with water, dried over Na_2SO_4 and roto-evaporated. The crude product was purified by column chromatography (eluent – hexane/AcOEt 4:1) to afford 270 mg (71%) of 3-(3-nitro-4-(phenylsulfonyl)phenyl)pyridine **19**. Iron powder (222 mg, 3.97 mmol) was added to a suspension of 270 mg (0.79 mmol) of compound **19** in 2.5 mL of AcOH. The mixture was stirred at 70 °C for 3 h and then cooled down and filtered. The precipitate was washed with AcOEt. The filtrate was diluted with water and extracted with AcOEt. The extract was washed with saturated $NaHCO_3$ solution, dried over Na_2SO_4 and roto-evaporated to afford 145 mg (59%) of 2-(phenylsulfonyl)-5-(pyridin-3-yl)aniline **21**. A solution of 120 mg (0.39 mmol) of compound **21** in 2 mL formic acid was refluxed for 3 h. The solvent was stripped in vacuo and the residue was treated with saturated $NaHCO_3$ solution, filtered, washed with water and dried in vacuo to afford 115 mg (87%) of *N*-(2-(phenylsulfonyl)-5-(pyridin-3-yl) phenyl)formamide **23**. A solution of borane dimethyl sulfide complex (2 M in THF, 0.49 mL, 0.98 mmol) was added to a solution of 110 mg (0.33 mmol) of compound **23** in 2 mL of THF and the mixture was stirred at ambient temperature for 12 h under Ar. The solution was quenched with saturated $NaHCO_3$ solution and extracted with DCM. The extract was dried over Na_2SO_4 and roto-evaporated. The crude product was purified by column chromatography (eluent–hexane/AcOEt 4:1) to afford 52 mg (49%) of compound **10h**. LS MC *m*/*z* 325 (M+1). ^{1}H NMR (DMSO-d_6, 400 MHz) δ 8.90 (s, 1H), 8.60 (s, 1H), 8.01 (m, 4H), 7.60 (m, 4H), 7.06 (d, J = 8.0 Hz, 1H), 6.93 (s, 1H), 6.50 (s, 1H), 2.89 (s, 3H).

N-Methyl-4-(phenylsulfonyl)biphenyl-3-amine **10i**. This compound was synthesized according to the procedure for compound **10h** from 4-iodo-2-nitro-1-(phenylsulfonyl)benzene **17** and phenylboronic acid. LS MC *m*/*z* 324 (M+1). ^{1}H NMR (DMSO-d_6, 400 MHz) δ 7.94 (m, 3H), 7.58 (m, 3H), 7.46 (m, 5H), 6.96 (dd, J_1 = 8.4 Hz, J_2 = 1.6 Hz, 1H), 6.83 (s, 1H), 6.45 (m, 1H), 2.93 (d, J = 4.8 Hz, 3H).

1-(4-(Phenylsulfonyl)phenyl)piperazine) **10j**.[23] A mixture of 5.64 g (40 mmol) of 1-fluoro-4-nitrobenzene **25** and 6.5 g (40 mmol) of sodium phenylsulfinate in 100 mL of DMF was stirred for 12 h at 120 °C. After cooling, the mixture was poured into 300 mL of water. The formed precipitate was filtered, washed with water and dried in vacuo. Yield was 9 g (86%) of compound **26**. ^{1}H NMR (DMSO-d_6, 400 MHz) δ 8.39 (d, J = 8.8 Hz, 2H), 8.23 (d, J = 8.8 Hz, 2H), 8.02 (d, J = 7.6 Hz, 2H), 7.75 (t, J = 7.6 Hz, 1H), 7.66 (t, J = 7.6 Hz, 2H). A mixture of 1 g (3.8 mmol) of compound **26** and 0.1 g of 10% Pd/C in 100 mL of methanol was stirred for 12 h under hydrogen. The solution was filtered through celite and roto-evaporated. The residue was dissolved in 50 mL of EtOAc and precipitated with 50 mL of hexane, filtered and dried in vacuo. Yield was 0.68 g (77%) of compound **27**. LS MC *m*/*z* 234 (M+1). ^{1}H NMR (DMSO-d_6, 400 MHz) δ 7.82 (d, J = 7.2 Hz, 2H), 7.55 (m, 5H), 6.61 (d, J = 8.4 Hz, 2H), 6.16 (s, 2H). A solution of 0.68 g (3 mmol) of 4-(phenylsulfonyl)aniline **27** in 4.2 mL of water and 0.42 mL of H_2SO_4 was cooled to 0 °C with stirring and a solution of 0.21 g (3.04 mmol) of $NaNO_2$ in 1 mL of water was added dropwise. The temperature was kept below 5 °C. After 30 min of stirring, a solution of 0.9 g (5.4 mmol) of K_i in 3.6 mL of water was added, and the stirring continued for 3 h. The mixture was extracted with ether. The extract was washed with 10% HCl, then with saturated $NaHCO_3$ solution and, finally, with a $Na_2S_2O_3$ solution and then dried over Na_2SO_4 and roto-evaporated. The crude product was purified by column chromatography (eluent–hexane/AcOEt 2:1) to afford 0.4 g (40%) of compound **28**. ^{1}H NMR (DMSO-d_6, 400 MHz) δ 8.01 (d, J = 8.4 Hz, 2H), 7.95 (d, J = 7.6 Hz, 2H), 7.71 (m, 3H), 7.63 (t, J = 7.6 Hz, 2H). A mixture of 0.4 g (1 mmol) of 1-iodo-4-(phenylsulfonyl)benzene **28**, 0.4 g (4.7 mmol) of piperazine, 0.19 g (17 mmol) of sodium *tert*-butoxide and 28 mg (0.036 mmol) of dichlorobis(tri-*o*-tolylphoCPhine)palladium (II) in 9 mL of dry toluene was refluxed under Ar for 12 h. The cooled mixture was filtered through celite and roto-evaporated. The product was isolated by HPLC. The yield was 23 mg (6%) of **10j**. LS MC *m*/*z* 303 (M+1).

N,N-Dimethyl-2-(phenylsulfonyl)-5-(piperazin-1-yl)aniline hydrochloride **10k**·HCl. A mixture of 209 mg (0.5 mmol) of compound **29**, 0.37 mL (5 mmol) of formalin and 21 mg of PtO_2 in 2 mL of methanol was stirred under hydrogen for 12 h. The mixture was filtered through celite, roto-evaporated, and the crude product was purified by HPLC. The obtained compound was dissolved in methanol, treated with an excess of 3 M HCl in dioxane and diluted with ether. The formed precipitate was filtered, washed with ether and dried in vacuo to afford 32 mg (19%) of compound **10k**·HCl. LS MC *m*/*z* 346 (M+1). ^{1}H NMR (DMSO-d_6, 400 MHz) δ 9.40 (br s, 3H), 7.88 (d, J = 8.8 Hz, 1H), 7.75 (d, J = 7.2 Hz, 2H), 7.59 (t, J = 7.2 Hz, 1H), 7.51 (t, J = 8.0 Hz, 2H), 6.91 (d, J = 8.8 Hz, 1H), 6.86 (s, 1H), 3.55 (m, 4H), 3.15 (m, 4H), 2.34 (s, 6H).

5-(Piperazine-1-yl)-2-(phenylsulfonyl)aniline hydrochloride **10l**·HCl. A 5 mL aliquot of TFA was added at 0 °C to a solution of 215 mg (0.52 mmol) of compound **29**[32] in 5 mL of DCM, and the solution was stirred at 0 °C for 2 h. The mixture was roto-evaporated, dissolved in methanol, treated with an excess of a 3 M HCl solution in dioxane and diluted with ether. The formed precipitate was filtered, washed with ether and dried under vacuum to afford 133 mg (73%) of compound **10l**·HCl. LS MC *m*/*z* 318 (M+1). ^{1}H NMR (DMSO-d_6, 400 MHz) δ 9.28 (br s, 2H), 7.86 (m, 2H), 7.62 (m, 1H), 7.55 (m, 2H), 7.51 (d, J = 9.2 Hz, 1H), 6.38 (dd, J_1 = 9.2 Hz, J_2 = 1.6 Hz, 1H), 6.22 (d, J = 1.6 Hz, 1H), 5.98 (brs, 2H), 3.41 (m, 4H), 3.14 (m, 4H).

N-Methyl-2-(phenylsulfonyl)-5-(piperazin-1-yl)aniline hydrochloride **10m**·HCl. A mixture of 208 mg (0.5 mmol) of compound **29**, 0.26 g of a 50% NaOH solution, 53 mk L (0.55 mmol) of dimethylsulfate, 10 mg (0.033 mmol) of tetrabutylammonium bromide and 2.2 mL of toluene was stirred intensively for 12 h. Then, 2 mL of 5% HCl solution was added, and the mixture was extracted with DCM. The organic extract was dried over Na_2SO_4 and roto-evaporated. The crude product was purified by HPLC to afford 35 mg (16%) of compound **30**. It was dissolved in 1 mL of DCM, 1 mL of TFA was added at 0 °C and the solution was stirred at 0 °C for 2 h. The mixture was roto-evaporated, dissolved in methanol, treated with access of 3 M HCl in dioxane and diluted with ether. The formed precipitate was filtered, washed with ether and dried in vacuum to afford 25 mg (85%) of compound **10m**·HCl. LS MC *m*/*z* 332 (M+1). ^{1}H NMR (DMSO-d_6, 400 MHz) δ 9.34 (br s, 2H), 7.87 (d, J = 7.6 Hz, 2H), 7.58 (m, 4H), 6.37 (d, J = 9.2 Hz, 1H), 5.99 (s, 1H), 3.52 (m, 4H), 3.14 (m, 4H), 2.78 (s, 3H).

N-Acetyl-2-(phenylsulfonyl)-5-(piperazin-1-yl)aniline hydrochloride **10n**·HCl. A mixture of 42 mg (0.1 mmol) of compound **25** and 0.15 mL of acetic anhydride was stirred at 0 °C under Ar for 1 h. The mixture was diluted with 0.5 mL of toluene and roto-evaporated. The residue was dissolved in AcOEt and precipitated with ether. The precipitate was filtered, washed with ether and dried in vacuo to obtain 38 mg (83%) of compound **31**. A solution of 24 mg (0.052 mmol) of compound **31** in 1 mL of DCM at 0 °C was treated with 0.6 mL of TFA and stirred at 0 °C for 2 h. The mixture was roto-evaporated, dissolved in methanol, treated with an excess of 3 M HCl in dioxane and diluted with ether. The formed precipitate was filtered, washed with ether and dried under vacuum to afford 17.5 мг (93.5%) of compound **10n**·HCl. LS MC *m*/*z* 360 (M+1). ^{1}H NMR (DMSO-d_6, 400 MHz) δ 9.41 (br s, 1H), 9.22 (br s, 2H), 7.87 (d, J = 8.8 Hz, 1H), 7.83 (d, J = 7.6 Hz, 1H), 7.66 (t, J = 7.6 Hz, 1H), 7.59 (t, J = 7.6 Hz, 2H), 7.41 (m, 1H), 6.94 (dd, J_1 = 9.2 Hz, J_2 = 2.8 Hz, 1H), 3.52 (m, 4H), 3.17 (m, 4H), 2.05 (s, 3H).

4.2. Biological assays

4.2.1. 5-HT$_6$ Receptor functional assay

5-HT$_6$R was sub-cloned into the T-REx system (Invitrogen, Carlsbad, CA) and expressed in HEK (5-HT$_6$R-HEK) cells. Cells were grown in DMEM supplemented with 10% FBS, 1% AAS, blasticidin S, and zeocin (all from Invitrogen, Carlsbad, CA) in a T-175 cell culture flask. T-REx/5-HT$_6$ receptor expression was activated by addition of tetracycline (1 μg/mL) a day before the experiments, as recommended by the T-REx system manufacturer (Invitrogen, Carlsbad, CA). On the day of the experiment, the cells were harvested from the flask using a 6 mM EDTA/HBSS solution, gently triturated by passing through a pipette tip several times to break down cell aggregates, washed with serum-free medium, and counted. The cells were resuspended to 0.67×10^6 cells/mL in SB2 buffer, HBSS and supplemented with 5 mM HEPES, pH 7.4, 0.05% BSA, and 1 mM IBMX (Sigma–Aldrich, St. Louis, MO) containing Alexa Fluor 647-anti cAMP antibody (from LANCE cAMP 384 kit, Perkin–Elmer, Waltham, MA). Then, 6 μL (~4000 cells/well) aliquots were transferred into 384-well assay plates (PerkinElmer White OptiPlates). The test compounds at different concentrations were premixed with serotonin hydrochloride (Sigma, MO) and added to the cells (final serotonin concentration 10 nM, final DMSO concentration 0.32%, final IBMX concentration 500 mM). Each assay plate contained serotonin and cAMP standard concentration curves. After 2 h of incubation with the mixture of compound/serotonin, the cells were treated as described in the cAMP LANCE assay kit protocol (PerkinElmer, Waltham, MA). The LANCE signal was measured using the multimode plate reader, VICTOR 3 (PerkinElmer, Waltham, MA), with built-in settings for the LANCE detection.

4.2.2. Curve fitting and determination of K_i

The concentration-dependent cell responses were fitted with Prism 5 (Graph-Pad, CA) using built-in 4-parametric equations to calculate IC_{50} values. All experiments were performed in duplicate. Standard deviations (SD) were calculated using Prism's built-in statistical package.

K_i values for functional 5-HT$_6$ receptor inhibition assays were calculated using Cheng-Prusoff's[41] modified equation:

$K_i = IC_{50}/(1 + [Ag]/EC_{50})$, where IC_{50} is the concentration of antagonist causing 50% inhibition of serotonin-induced cell response; [Ag] is a concentration of serotonin (10 nM), at which inhibition was measured; and EC_{50} is serotonin concentration causing 50% stimulation of the cell response measured simultaneously with the test compounds. The mean EC_{50} value for serotonin-induced cAMP production in 5-HT$_6$R-HEK cells was 1.91 ± 0.13 nM as determined from four independent experiments (different days) with three to five repeats (separate plates) each day, performed in quadruplicates on each plate.

Acknowledgment

The authors thank Dr. Norman Lee from the Chemical Instrumentation Center, Boston University, for HRMS measurements.

Supplementary data

Supplementary data associated with this article can be found, in the online version, at http://dx.doi.org/10.1016/j.bmc.2013.05.040. These data include MOL files and InChiKeys of the most important compounds described in this article.

References and notes

1. *Int. Rev. Neurobiol. Pharmacology of 5-HT6 receptors, Part I*; Borsini, F., Ed.; Academic Press, 2010; Vol. 94,
2. *Int. Rev. Neurobiol. Pharmacology of 5-HT6 receptors, Part II*; Borsini, F., Ed.; Academic Press, 2010; Vol. 96,
3. Marsden, C. A.; King, M. V.; Fone, K. C. *Neuropharmacology* **2011**, *61*, 400.
4. Marazziti, D.; Baroni, S.; Dell'Osso, M. C.; Bordi, F.; Borsini, F. *Curr. Med. Chem.* **2011**, *18*, 2783.
5. Codony, X.; Vela, J. M.; Ramirez, M. J. *Curr. Opin. Pharmacol.* **2011**, *11*, 94.

6. Ivachtchenko, A. V.; Ivanenkov, Y. A.; Tkachenko, S. E. *Expert Opin. Ther. Patents* **2010**, *20*, 1171.
7. Ivachtchenko, A. V.; Ivanenkov, Y. A. *Expert Opin. Ther. Patents* **2012**, *22*, 917.
8. Ivachtchenko, A. V.; Ivanenkov, Y. A.; Skorenko, A. V. *Expert Opin. Ther. Patents* **2012**, *22*, 1123.
9. Holenz, J.; Merce, R.; Dıaz, J. L.; Guitart, X.; Codony, X.; Dordal, A.; Romero, G.; Torrens, A.; Mas, J.; Andaluz, B.; Hernandez, S.; Monroy, X.; Sanchez, E.; Hernandez, E.; Perez, R.; Cubi, R.; Sanfeliu, O.; Buschmann, H. *J. Med. Chem.* **2005**, *48*, 1781.
10. Lopez-Rodriguez, M. L.; Benhamu, B.; de la Fuente, T.; Sanz, A.; Pardo, L.; Campillo, M. *J. Med. Chem.* **2005**, *48*, 4216.
11. Ivachtchenko, A. V.; Dmitriev, D. E.; Golovina, E. S.; Dubrovskaya, E. S.; Kadieva, M. G.; Koryakova, A. G.; Kysil, V. M.; Mitkin, O. D.; Tkachenko, S. E.; Okun, I. M.; Vorobiov, A. A. *Bioorg. Med. Chem. Lett.* **2010**, *20*, 2133.
12. Ivachtchenko, A. V.; Golovina, E. S.; Kadieva, M. G.; Koryakova, A. G.; Mitkin, O. D.; Tkachenko, S. E.; Kysil, V. M.; Okun, I. *Eur. J. Med. Chem.* **2011**, *46*, 1189.
13. Wu, Y.-J.; He, H.; Hu, S.; Huang, Y.; Scola, P. M.; Grant-Young, K.; Bertekap, R. L.; Wu, D.; Gao, Q.; Li, Y.; Klakouski, C.; Westphal, R. S. *J. Med. Chem.* **2003**, *46*, 4834.
14. Jacobsen, J. E.; King, S. J. Bis-arylsulfones. Int. Pat. Appl. WO 200,1098,279, 2001.
15. Ivachtchenko, A. V.; Golovina, E. S.; Kadieva, M. G.; Kysil, V. M.; Mitkin, O. D.; Vorobiov, A. A.; Okun, I. *Bioorg. Med. Chem. Lett.* **2012**, *22*, 4273.
16. Kim, H.-J.; Doddareddy, M. R.; Choo, H.; Cho, Y. S.; No, K. T.; Park, W.-K.; Pae, A. N. *J. Chem. Inf. Model.* **2008**, *48*, 197.
17. Upton, N.; Chuang, T. T.; Hunter, A. J.; Virley, D. J. *Neurotheraphy* **2008**, *5*, 458.
18. Maher-Edwards, G.; Zvartau-Hind, M.; Hunter, A. J.; Gold, M.; Hopton, G.; Jacobs, G.; Davy, M.; Williams, P. *Curr. Alzheimer Res.* **2010**, *7*, 374.
19. Turner, S. C.; Braje, W.; Haupt, A.; Lange, U.; Drescher, K.; Wicke, K.; Unger, L.; Mezler, M.; Wernet, W.; Mayrer, M. WO 2,009,019,286, 2009, patentscope.wipo.int/search/en/detail.jsf?docId=WO2009019286.
20. Holenz, J.; Pauwels, P. J.; Diaz, J. L.; Merce, R.; Codony, X.; Buschman, H. *Drug Discovery Today* **2006**, *11*, 283.
21. Ivachtchenko, A. V.; Golovina, E. S.; Kadieva, M. G.; Kysil, V. M.; Mitkin, O. D.; Tkachenko, S. E.; Okun, I. M. *Bioorg. Med. Chem.* **2011**, *19*, 1482.
22. Zhu, W.; Ma, D. *J. Org. Chem.* **2005**, *70*, 2696.
23. Sikazwe, D.; Bondarev, M. L.; Dukat, M.; Rangisetty, J. B.; Roth, B. L.; Glennon, R. A. *J. Med. Chem.* **2006**, *49*, 5217.
24. Hirst, W. D.; Abrahamsen, B.; Blaney, F. E.; Calver, A. R.; Aloj, L.; Price, G. W.; Medhurst, A. D. *Mol. Pharmacol.* **2003**, *64*, 1295.
25. Su, W. *Tetrahedron Lett.* **1994**, *35*, 4955.
26. Betebenner, D. A.; Degoey, D. A.; Maring, C. J.; Krueger, A. C.; Iwasaki, N.; Rockway, T. W.; Cooper, C. S.; Anderson, D. D.; Donner, P. L.; Green, B. E.; Kempe, D. J.; Liu, D.; Mcdaniel, K. F.; Madigan, D. L.; Motter, C. E.; Pratt, J. K.; Shanley, J. P.; Tufano, M. D.; Wagner, R.; Zhang, R.; Molla, A.; Mo, H.; Pilot-Matias, T. J.; Masse, S. V.; Carrick, R. J.; He, W.; Lu, L.; Grampovnik, D. J. WO 2007/081517, 2007, patentscope.wipo.int/search/en/detail.jsf?docId=WO2007081517.
27. Courtin, A.; Tobel, H.-R.; Auerbach, G. *Helv. Chim. Acta* **1980**, *63*, 1412.
28. Castro, P. J. L.; Cooper, L. C.; Gilligan, M.; Humphries, A. C.; Hunt, P. A.; Ladduwahetty, T.; Macleod, A. M.; Merchant, K. J.; Van Niel, M. B.; Wilson, K. WO 2006/021805, 2006, patentscope.wipo.int/search/en/detail.jsf?docId=WO2006021805.
29. Bossio, R.; Marcaccini, S.; Pepino, R.; Torroba, T. *Heterocycles* **1996**, *43*, 471.
30. Feutrill, G. I.; Mirrington, R. N. *Aust. J. Chem.* **1973**, *26*, 357.
31. Crawford, J. J.; Dossetter, A. G.; Finlayson, J. E.; Heron, N. M. WO 200,901,127, 2008, patentscope.wipo.int/search/en/detail.jsf?docId=WO2009001127.
32. Jacobsen, E. J.; King, S. J. US Pat. Appl. U.S. 2004/0014966 A1, 2004, www.google.com/patents/US20040014966.
33. Teller, D. C.; Okada, T.; Behnke, C. A.; Palczewski, K.; Stenkamp, R. E. *Biochemistry* **2001**, *40*, 7761.
34. Okada, T.; Sugihara, M.; Bondar, A. N.; Elstner, M.; Entel, P.; Buss, V. *J. Mol. Biol.* **2004**, *342*, 571.
35. Rasmussen, S. G.; Choi, H. J.; Rosenbaum, D. M.; Kobilka, T. S.; Thian, F. S.; Edwards, P. C.; Burghammer, M.; Ratnala, V. R.; Sanishvili, R.; Fischetti, R. F.; Schertler, G. F.; Weis, W. I.; Kobilka, B. K. *Nature* **2007**, *450*, 383.
36. Chien, E. Y.; Liu, W.; Zhao, Q.; Katritch, V.; Han, G. W.; Hanson, M. A.; Shi, L.; Newman, A. H.; Javitch, J. A.; Cherezov, V.; Stevens, R. C. *Science* **2010**, *330*, 1091.
37. Jaakola, V. P.; Griffith, M. T.; Hanson, M. A.; Cherezov, V.; Chien, E. Y.; Lane, J. R.; Ijzerman, A. P.; Stevens, R. C. *Science* **2008**, *322*, 1211.
38. Wu, B.; Mol, C. D.; Han, G. W.; Katritch, V.; Chien, E. Y. T.; Liu, W.; Cherezov, V.; Stevens, R. C. *Science* **2010**, *330*, 1066.
39. Hao, M.; Li, Y.; Li, H.; Zhang, S. *Int. J. Mol. Sci.* **2011**, *12*, 5011.
40. Okun, I. M.; Tkachenko, S. E.; Khvat, A.; Mitkin, O.; Kazey, V.; Ivachtchenko, A. V. *Curr. Alzgeimer Res.* **2010**, *7*, 97.
41. Cheng, Y.; Prusoff, W. H. *Biochem. Pharmacol.* **1973**, *22*, 3099.
42. Ivachtchenko, A. V.; Golovina, E. S.; Kadieva, M. G.; Kysil, V. M.; Mitkin, O. D.; Tkachenko, S. E.; Okun, I. M. *J. Med. Chem.* **2011**, *54*, 8161.
43. Ivachtchenko, A. V.; Golovina, E. S.; Kadieva, M. G.; Kysil, V. M.; Mitkin, O. D.; Vorobiev, A. A.; Okun, I. *Bioorg. Med. Chem. Lett.* **2012**, *22*, 4273.
44. Ivachtchenko, A. V.; Dmitriev, D. E.; Golovina, E. S.; Kadieva, M. G.; Koryakova, A. G.; Kysil, V. M.; Mitkin, O. D.; Okun, I. M.; Tkachenko, S. E.; Vorobiev, A. A. *J. Med. Chem.* **2010**, *53*, 5186.
45. Ahmed, M.; Johnson, C. N.; Jones, M. C.; MacDonald, G. J.; Moss, S. F.; Thompson, M.; Wade, C. E.; Witty, D. WO 2003/080580, 2003, patentscope.wipo.int/search/en/detail.jsf?docId=WO2003080580.